



Journal of Aerospace Technology and
Management

ISSN: 1984-9648

editor@jatm.com.br

Instituto de Aeronáutica e Espaço
Brasil

Song, Xiaoke; Guo, Hongwei; Liu, Rongqiang; Deng, Zongquan
Structure Synthesis and Optimization of Feed Support Mechanisms for a Deployable
Parabolic Antenna
Journal of Aerospace Technology and Management, vol. 8, núm. 1, enero-marzo, 2016,
pp. 1-9
Instituto de Aeronáutica e Espaço
São Paulo, Brasil

Available in: <http://www.redalyc.org/articulo.oa?id=309443498006>

- How to cite
- Complete issue
- More information about this article
- Journal's homepage in redalyc.org

redalyc.org

Scientific Information System

Network of Scientific Journals from Latin America, the Caribbean, Spain and Portugal

Non-profit academic project, developed under the open access initiative

Structure Synthesis and Optimization of Feed Support Mechanisms for a Deployable Parabolic Antenna

Xiaoke Song¹, Hongwei Guo¹, Rongqiang Liu¹, Zongquan Deng¹

ABSTRACT: In this paper, a systematic method to synthesize parallel mechanisms for feed support mechanisms based on screw theory is proposed. First, the motion requirement of the feed support mechanism is studied. Then, a class of parallel mechanisms having a translational motion with different degrees of freedom is synthesized based on the constraint-synthesis method. Then, these parallel mechanisms are modified based on the specificities of deployable mechanisms, and two kinds of mechanisms are selected as the unit for the feed support mechanism. Finally, the deployment ratio of two kinds of mechanisms is optimized. The configurations obtained in this paper can enrich the types of feed support mechanisms.

KEYWORDS: Feed support mechanism, Deployable mechanism, Structure synthesis, Deployment ratio, Parallel mechanism, Screw theory.

INTRODUCTION

Large deployable parabolic antennas are widely used on the aerospace equipment with the development of satellite communication technology (Sauder and Thomson 2014; Cherniavsky *et al.* 2004; Yurduseven *et al.* 2012). They are composed of parabolic reflector, feed, feed support mechanism, and so on. There are positive and offset feed for the position of the feed in the parabolic antenna. The position accuracy concerns the properties of the antennas (Tayebi *et al.* 2013; Pour *et al.* 2014; Silver 1949). Thus, for the feed support mechanism, it should present high precision, high stiffness, large deployment ratio, simple structure etc. At present, there are several types of feed support mechanisms, such as robot arm, static truss and so on (Sauder and Thomson 2014).

This paper studies the feed support mechanism of an inflatable deployable parabolic antenna. As the support of the feed, the mechanism takes it to a predetermined position, so the mechanism only needs to carry out the translation motion in one dimension. Based on the requirements on the feed support mechanisms and the advantages of parallel mechanisms, such as high precision and high rigidity (Merlet 2006; Tsai 1999), we select the one dimensional parallel mechanisms as the research object and take structure synthesis and optimization for it. Regarding the structure synthesis of the parallel mechanism, lots of achievements have been obtained. Fang and Tsai (2002), Huang and Li (2002) and Xu *et al.* (2012) have used the screw theory to synthesize lots of parallel mechanisms. Li *et al.* (2004) synthesized the 3R2T 5DOF parallel mechanisms by Lie group. Gao *et al.* (2011) synthesized the parallel mechanisms with two

¹Harbin Institute of Technology – State Key Laboratory of Robotics and System – Harbin/Heilongjiang – China.

Author for correspondence: Hongwei Guo | Yikuang Street 2, Nangang District | Harbin/Heilongjiang – China | Email: ghwhit@163.com

Received: 09/17/2015 | Accepted: 11/23/2015

dimensional rotations. In this study, we have chosen screw theory to synthesize the parallel mechanisms.

The rest of this paper is organized as follows. Firstly, the inflatable deployable parabolic antenna is introduced, and the requirement of the feed support mechanism is given. Following, the constraint-synthesis method based on screw theory is briefly introduced. Then, the structure synthesis of the mechanism is carried out. The resulted structures are modified and one suitable type is selected. The deployment ratio of the selected structure is optimized next. At last, a conclusion is given.

MOTION REQUIREMENT FOR THE FEED SUPPORT MECHANISM

Figure 1 shows the studied inflatable deployable parabolic antenna. The antenna has two forms: folded and deployed. Regarding the feed support mechanism, it is composed of several deployable units serially connected. The unit should output a translation along the z -axis. It can also have motions in other directions. As parallel mechanisms have the advantages of high stiffness and high precision, we selected parallel mechanisms as the unit. Based on the experience of practical engineering, we focused on the synthesis of parallel mechanisms with the degree of freedom (DOF) of $1T^z$, $1T^z1R^z$, and $1T^z2R^{xy}$ (the numbers before T and R denote the number of DOF; T and R denote the translational and rotational freedom separately; the right superscripts denote the direction of the motion). Because of the difficulties in driving and locking prismatic joints, we only used revolute joints in the structure synthesis. Therefore, we considered the structure synthesis for parallel mechanisms with the DOF of $1T^z$, $1T^z1R^z$, and $1T^z2R^{xy}$, which have only revolute joints.

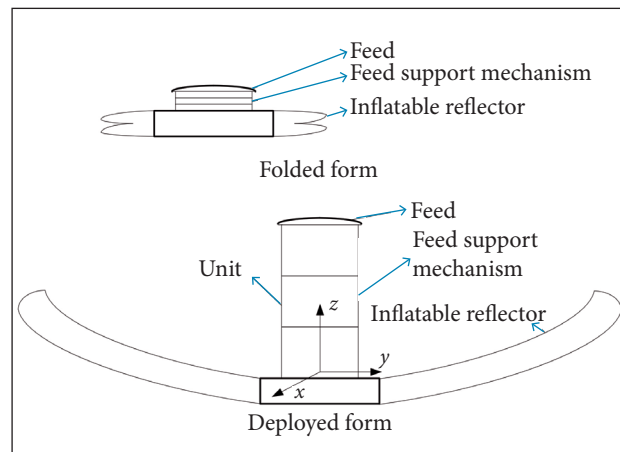


Figure 1. The inflatable deployable parabolic antenna.

BASIC CONCEPTS AND THE CONSTRAINT-SYNTHESIS METHOD

In screw theory, a unit screw is defined as below:

$$\mathcal{S} = (\mathbf{s}; \mathbf{s}_0) = (\mathbf{s}; \mathbf{r} \times \mathbf{s} + h\mathbf{s}) \quad (1)$$

where: \mathbf{s} is a unit vector and denotes the direction of the screw axis; \mathbf{r} is the position vector of any point on the screw axis; h is the pitch of the screw.

For a screw, $\mathcal{S}^r = (\mathbf{s}_r; \mathbf{s}_{0r})$, and a set of screws, $\mathcal{S}_1, \mathcal{S}_2, \dots, \mathcal{S}_n$, they are said to be reciprocal if they satisfy the condition:

$$\mathcal{S}_j \circ \mathcal{S}^r = \mathbf{s}_j \cdot \mathbf{s}_{0r} + \mathbf{s}_r \cdot \mathbf{s}_{0j} = 0 \quad (j = 1, 2, \dots, n) \quad (2)$$

where: \circ represents the reciprocal product; \mathcal{S}_j represents the j -th screw.

We call the screw a twist if it represents an instantaneous motion of a rigid body. We call the screw a wrench if it represents a force and a coaxial couple acting on a rigid body. A force or a rotation can be given by $(\mathbf{s}; \mathbf{r} \times \mathbf{s})$, and a couple or a translation can be given by $(0; \mathbf{s})$. In the synthesis process, the prismatic joint (P) outputs a translation, and the revolute joint (R) outputs a rotation. Other types of joints can be expressed as the combination of the two basic joints. For example, the spherical joint (S) can be expressed as three R joints intersecting at a point, but they are not coplanar; the universal joint (U) can be expressed as two intersecting R joints; the cylindrical joint (C) can be expressed as a P joint and a R joint which are concentric.

For the parallel mechanisms, if a set of screws represent the twists of one limb, then its reciprocal screws, $\mathcal{S}_1^r, \mathcal{S}_2^r, \dots, \mathcal{S}_n^r$ ($n < 6$) represent the constraint wrenches the limb exerted on the moving platform. Thus the combination of these reciprocal screws of all limbs determines the constraints of the moving platform, and the motion twists of the moving platform are reciprocal to the combination of the constraint wrenches. This is the mathematical basis for the constraint-synthesis method.

The process of the structure synthesis by constraint-synthesis method is shown as follows. First, the motion twists are obtained based on the motion requirement of the mechanism, then we get the constraint wrenches of the moving platform, which are reciprocal to the motion twists. Next, we distribute the constraint wrenches to each limb. Thus we get the motion twists of each limb based on the constraint wrenches of the limb, as they are reciprocal, then construct the limb kinematic chain based on the motion twists. Finally, we assemble the limbs in

proper configuration to guarantee that the combination of the limb constraint wrenches of each limb is equal to the constraint wrenches of moving platform.

STRUCTURE SYNTHESIS OF PARALLEL MECHANISMS FOR FEED SUPPORT MECHANISMS

The feed support mechanism is used to support the feed of antennas; it would suffer the interference from every direction, so the mechanism should have roughly the same load capacity on every direction. According to the experience on practical engineering and the load of feed support mechanisms, the mechanism should have three or four limbs, as more limbs make the manufacturing complicated and less limbs cannot get the uniform load capacity. So the objective in this study is to synthesize parallel mechanisms with three or four limbs composed of only revolute joints.

For the parallel mechanisms with one DOF of $1T^z$, the twist system of the moving platform is represented as:

$$\mathcal{S}_1 = (0 \ 0 \ 0; \ 0 \ 0 \ 1) \quad (3)$$

From Eq. 2, the constraint wrench system which is reciprocal to the twist system is obtained as:

$$\begin{aligned} \mathcal{S}_1^r &= (1 \ 0 \ 0; \ 0 \ 0 \ 0) \\ \mathcal{S}_2^r &= (0 \ 1 \ 0; \ 0 \ 0 \ 0) \\ \mathcal{S}_3^r &= (0 \ 0 \ 0; \ 1 \ 0 \ 0) \\ \mathcal{S}_4^r &= (0 \ 0 \ 0; \ 0 \ 1 \ 0) \\ \mathcal{S}_5^r &= (0 \ 0 \ 0; \ 0 \ 0 \ 1) \end{aligned} \quad (4)$$

which represents two constraint forces whose direction is parallel to the x -axis and y -axis separately and three constraint couples whose direction is parallel to the x -axis, y -axis, and z -axis separately.

Then we get the constraint wrench system of mechanisms with DOF of $1T^z1R^z$ and $1T^z2R^{xy}$ in the same way, just as Eqs. 5 and 6.

$$\begin{aligned} \mathcal{S}_1^r &= (1 \ 0 \ 0; \ 0 \ 0 \ 0) \\ \mathcal{S}_2^r &= (0 \ 1 \ 0; \ 0 \ 0 \ 0) \\ \mathcal{S}_3^r &= (0 \ 0 \ 0; \ 1 \ 0 \ 0) \\ \mathcal{S}_4^r &= (0 \ 0 \ 0; \ 0 \ 1 \ 0) \end{aligned} \quad (5)$$

$$\begin{aligned} \mathcal{S}_1^r &= (1 \ 0 \ 0; \ 0 \ 0 \ 0) \\ \mathcal{S}_2^r &= (0 \ 1 \ 0; \ 0 \ 0 \ 0) \\ \mathcal{S}_3^r &= (0 \ 0 \ 0; \ 0 \ 0 \ 1) \end{aligned} \quad (6)$$

Based on the reciprocal condition of screws, we then analyze the relation between a revolute joint and its constraint wrenches (Fang and Tsai 2002).

We define three unit screws, $\mathcal{S}_r = (\mathbf{w}; \mathbf{r}_1 \times \mathbf{w})$, $\mathcal{S}_f = (\mathbf{f}; \mathbf{r}_2 \times \mathbf{f})$, $\mathcal{S}_c = (0 \ 0 \ 0; \mathbf{c})$, to indicate the revolute joint, constraint force and constraint couple, respectively, where \mathbf{w} indicates the direction of the revolute joint; \mathbf{r}_1 indicates a point on the joint; \mathbf{f} indicates the direction of the constraint force; \mathbf{r}_2 indicates a point on the force; \mathbf{c} indicates the direction of constraint couple. As the reciprocal product of revolute joint and constraint force is zero, as well as the reciprocal product of revolute joint and constraint couple, we have Eqs. 7 and 8.

$$\begin{aligned} \mathcal{S}_r \circ \mathcal{S}_f &= \mathbf{w} \cdot (\mathbf{r}_2 \times \mathbf{f}) + \mathbf{f} \cdot (\mathbf{r}_1 \times \mathbf{w}) \\ &= \mathbf{r}_2 \cdot (\mathbf{f} \times \mathbf{w}) + \mathbf{r}_1 \cdot (\mathbf{w} \times \mathbf{f}) \\ &= (\mathbf{r}_2 - \mathbf{r}_1) \cdot (\mathbf{f} \times \mathbf{w}) \\ &= 0 \end{aligned} \quad (7)$$

From Eq. 7, we conclude that $\mathbf{r}_2 - \mathbf{r}_1 = 0$ or $\mathbf{f} \times \mathbf{w} = 0$, so $\mathbf{r}_2 = \mathbf{r}_1$ or $\mathbf{f} // \mathbf{w}$, that is to say, the axis of a revolute joint is parallel or intersects the constraint force.

$$\mathcal{S}_r \circ \mathcal{S}_c = \mathbf{w} \cdot \mathbf{c} = 0 \quad (8)$$

From Eq. 8, we conclude that $\mathbf{w} \perp \mathbf{c}$, that is to say, the axis of a revolute joint is perpendicular to the constraint couple.

For a kinematic chain with only revolute joints, the geometric condition of the revolute joints would change after motion, then the relation between revolute joints and constraints would change. So the mobility of the parallel mechanism composed of these kinematic chains would change. Only the revolute joints which are parallel or intersect at one point, or the chains composed of these two kinds of revolute joints, would keep their geometric conditions steady and their constraints would keep steady. These kinematic chains are shown in Fig. 2, where \mathbf{F} indicates the constraint force and \mathbf{C} indicates the constraint couple.

In these kinematic chains, there exist two kinds of revolute joints: the type-1 joints intersect at a common point and are not coplanar; the type-2 joints are parallel. According to the relation between revolute joint and its constraints, the geometric

condition and constraint wrenches of the kinematic chains are shown in Table 1.

In Table 1, the subscript numbers represent the type of revolute joints, and the superscript letters represent the axis to which the joints are parallel.

Using the kinematic chains shown above, we carry out the synthesis of the three kinds of mechanisms.

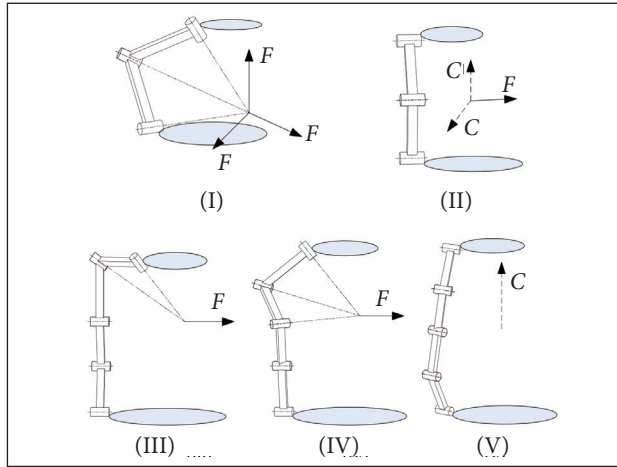


Figure 2. The kinematic chains with constant geometric conditions.

Table 1. The limbs with constant geometrical condition.

Limb type	Constraint wrenches	Denotation
I	Three forces passing through the central point which are not coplanar	$R_1 R_1 R_1$
II	One force parallel to the R joints; two couples perpendicular to the R joints which are not parallel	$R_2 R_2 R_2$
III	One force passing through the central point and parallel to the R joints	$R_1 R_1 R_2 R_2 R_2$
IV	One force passing through the central point and parallel to the R joints	$R_1 R_1 R_1 R_2 R_2$
V	One couple perpendicular to all the R joints	$R_2^A R_2^A R_2^A R_2^B R_2^B$

1T^z PARALLEL MECHANISMS

From the constraint-synthesis method, we know that the moving platform constraint system is the combination of all the limb constraint systems, so they can be derived from Eq. 4 and the relationship of constraint forces, couples, and constraint motion, just as shown in Table 2.

The mechanisms constructed in the mentioned ways are shown as follows.

In Fig. 3, the numbers i ($i = 1, 2, \dots$) indicate the number of the limb; F_i ($i = 1, 2, \dots$) indicate the constraint force which the limb i exerts on the mobile platform; C_i ($i = 1, 2, \dots$) indicate the constraint couple exerted by the limb i ; C_{ij} ($i = 1, 2, \dots; j = 1, 2, \dots$) indicate the constraint couple j which the limb i exerts on the mobile platform.

For the mechanism in Fig. 3a, F_1 and F_2 constrain the translations along the x - y -axes; C_{11} and C_{21} constrain the rotations around the x - y -axes; C_{12} and C_{22} are parallel and constrain the rotation around the z -axis, then the mechanism retains only one DOF of the translation along the z -axis.

For the mechanism in Fig. 3b, F_1 and F_2 are coplanar and intersect at the common point A , so they constrain two translations in the plane. As the plane is parallel to the base platform, the translations along the x - y -axes are constrained.

Table 2. The limbs of the 1T^z parallel mechanism.

Limb type	Limb number	Limb constraint	Geometric conditions
II	2	1 force and 2 couples	The type-2 revolute joints in two limbs are not parallel
III or IV	2	1 force	The central points of the type-1 revolute joints of the two limbs are coincident, and the type-2 revolute joints are parallel to the fixed base and not parallel between two limbs
V	3	1 couple	The three constraint couples C are not coplanar

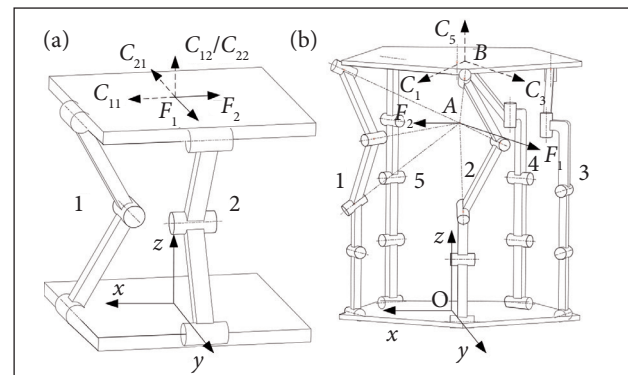


Figure 3. The parallel mechanisms with the DOF of 1T^z.

C_3 , C_4 , and C_5 are not coplanar and constrain three rotations in space. So the mechanism has only the DOF of translation along the z -axis.

The first mechanism is the Sarrus mechanism. It is widely used as deployable mechanisms with three or four limbs, such as the HIMAT. The other mechanism is too complicated to use as a deployable unit for the feed support mechanisms.

1T^z1R^z PARALLEL MECHANISMS

For the parallel mechanisms with the DOF of 1T^z1R^z, the moving platform is constrained with two forces and two couples. The constraint could be exerted by four limbs, two limbs of type III or IV and two limbs of type V, with each limb exerting a force or a couple. The limbs of the structures are shown in Table 3.

The mechanism constructed by the mentioned way is shown as follows.

For the mechanism in Fig. 4, as well as the analysis in the structure synthesis of 1T^z parallel mechanisms, F_1 and F_2 intersect

at the common point A , so they constrain two translations along the x - y -axes. C_3 and C_4 are coplanar and constrain the rotations around the x - y -axes. So the mechanism has the DOF of 1T^z1R^z.

1T^z2R^{xy} PARALLEL MECHANISMS

For the parallel mechanisms with DOF of 1T^z2R^{xy}, the constraint wrenches are composed of two forces along the x -axis and y -axis, respectively, and a couple around the z -axis. The constraints could be exerted by three kinematic limbs of type III or IV, where the three constraint forces are parallel to the fixed base and coplanar but do not intersect at a point. Or the constraints are exerted by two chains of type III or IV and one chain of type V, where the two constraint forces are parallel to the fixed base, intersect at a point, and the constraint couple is perpendicular to the fixed base. The constraint could also be exerted by four limbs, type III or IV, where the couple is exerted by two parallel forces. The detailed configuration is given in Table 4.

The mechanisms constructed in the mentioned way are shown in Fig. 5 as follows.

Table 3. The limbs of the 1T^z1R^z parallel mechanism.

Limb type	Limb number	Limb constraint	Geometric conditions
III or IV	2	1 force	The central points of the type-1 revolute joints of the two limbs are coincident. The type-2 revolute joints are parallel to the fixed base and not parallel between two limbs
V	2	1 couple	The constraint couples are parallel to the fixed base, but not parallel to each other.

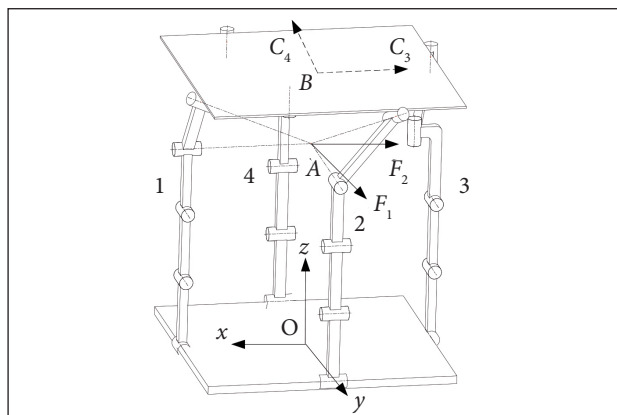


Figure 4. The parallel mechanisms with the DOF of 1T^z1R^z.

Table 4. The limbs of the 1T^z1R^{xy} parallel mechanism.

Limb type	Limb number	Limb constraint	Geometric conditions
III or IV	2	1 force	The central points of the two limbs are coincident. The type-2 revolute joints are parallel to the fixed base and not parallel between two limbs
V	1	1 couple	The constraint couples are perpendicular to the fixed base
III or IV	3	1 force	The central points of the three limbs are coplanar. The type-2 revolute joints of each group are parallel to the fixed base, but they are not parallel between different groups
III or IV	4	1 force	The four limbs are divided into two groups, each one with two limbs. The central points of the four limbs are coplanar. The type-2 revolute joints of each group are parallel, but they are not parallel between two groups

In Fig. 5, C_{i-j} ($i = 1, 2, \dots; j = 1, 2, \dots$) indicate the constraint couple exerted by two parallel constraint forces, F_i and F_j ; C_{i-j-k} ($i = 1, 2, \dots; j = 1, 2, \dots; k = 1, 2, \dots$) indicate the constraint couple exerted by three coplanar constraint forces, F_i , F_j and F_k .

For the mechanism in Fig. 5a, as well as the analysis in the structure synthesis of $1T^z$ and $1T^zR^{xy}$ parallel mechanisms, the constraint forces F_1 and F_2 intersect at the point A and they are parallel to the base platform, so they constrain the translations along x - y -axes. The constraint couple C_3 constrains the rotation around z -axis. So this mechanism has the DOF of $1T^z2R^{xy}$.

For the mechanism in Fig. 5b, F_1 , F_2 , and F_3 are coplanar and not parallel; besides, they do not intersect at a common point, so they exert a couple C_{1-2-3} to the mobile platform. The two translations in the plane and one rotation around the normal of the plane are constrained. As plane ABC is parallel to the base platform, the mechanism meets our requirements.

For the mechanism in Fig. 5c, F_1 and F_3 are parallel; F_2 and F_4 are parallel; F_1 , F_2 , F_3 , and F_4 are coplanar, so two couples, C_{1-3} and C_{2-4} , are exerted to the mobile platform and then the translations along x - y -axes and rotation around z -axis are constrained.

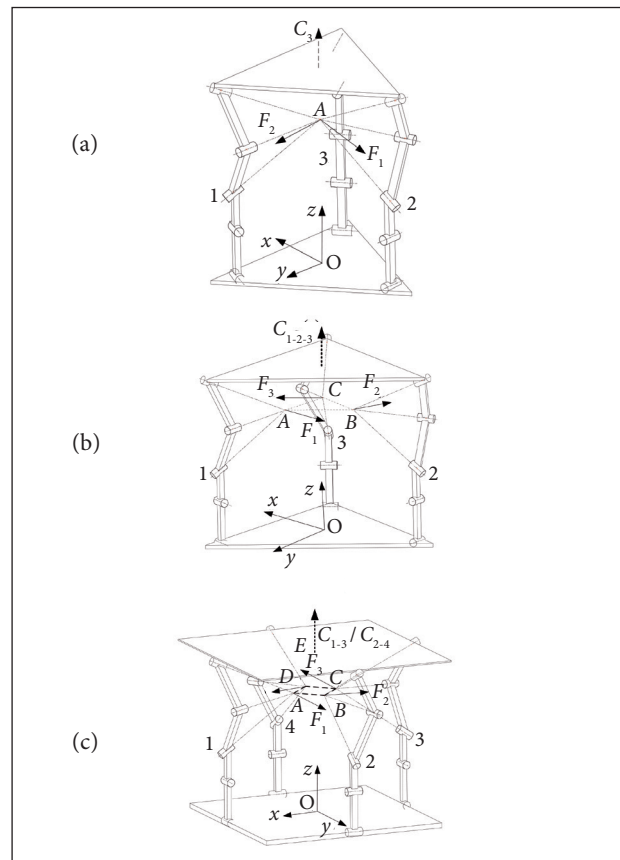


Figure 5. The parallel mechanisms with the DOF of $1T^z1R^{xy}$.

THE MODIFICATION OF THE PARALLEL MECHANISMS AND THE SELECTION OF THE DEPLOYABLE UNIT

For the feed support mechanism, the linkage in the limb of the mechanism should be as few as possible, in order to actuate and lock the mechanism easily. Based on the content of the basic concepts, two intersecting revolute joints compose a U joint, and three revolute joints which are intersecting but not coplanar compose a S joint. So we can use the U and S joints to substitute the revolute joints in special configuration to reduce the linkages. The result is shown in Table 5. Three mechanisms with the typical configurations, $3 - R_1U_{12}R_2R_2$, $3 - R_2R_2S$, and $4 - R_2R_2S$, are shown in Fig. 6.

Table 5. The mechanisms containing universal and spherical joints.

Mobility	Limb composed only of R joints	Limb composed of U and S joints
$1T^z$	$2 - R_2R_2R_2$	None
	$2 - R_1R_1R_2R_2R_2 - 3 - R_2^A R_2^A R_2^A R_2^B R_2^B$	$2 - R_1U_{12}R_2R_2 - 3 - R_2^A R_2^A U_{22}^{AB} R_2^B$
	$2 - R_1R_1R_1R_2R_2 - 3 - R_2^A R_2^A R_2^A R_2^B R_2^B$	$2 - R_1R_1U_{12}R_2 - 3 - R_2^A R_2^A U_{22}^{AB} R_2^B$
$1T^z1R^z$	$2 - R_1R_1R_1R_2R_2 - 2 - R_2^A R_2^A R_2^A R_2^B R_2^B$	$2 - R_1U_{12}R_2R_2 - 2 - R_2^A R_2^A U_{22}^{AB} R_2^B$
	$2 - R_1R_1R_2R_2R_2 - 2 - R_2^A R_2^A R_2^A R_2^B R_2^B$	$2 - R_1R_1U_{12}R_2 - 2 - R_2^A R_2^A U_{22}^{AB} R_2^B$
	$2 - R_1R_1R_2R_2R_2 - 1 - R_2^A R_2^A R_2^A R_2^B R_2^B$	$2 - R_1U_{12}R_2R_2 - 1 - R_2^A R_2^A U_{22}^{AB} R_2^B$
$1T^z2R^{xy}$	$2 - R_1R_1R_1R_2R_2 - 1 - R_2^A R_2^A R_2^A R_2^B R_2^B$	$2 - R_1R_1U_{12}R_2 - 1 - R_2^A R_2^A U_{22}^{AB} R_2^B$
	$3 - R_1R_1R_2R_2R_2$	$3 - R_1U_{12}R_2R_2, 3 - R_2R_2S$
	$3 - R_1R_1R_1R_2R_2$	$3 - R_1R_1U_{12}R_2$
	$4 - R_1R_1R_2R_2R_2$	$4 - R_1U_{12}R_2R_2$
	$4 - R_1R_1R_1R_2R_2$	$4 - R_1R_1U_{12}R_2, 4 - R_2R_2S$

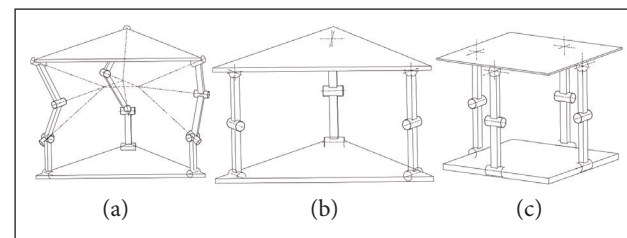


Figure 6. The 3-D model of parallel mechanisms $3 - R_1U_{12}R_2R_2$, $3 - R_2R_2S$, and $4 - R_2R_2S$.

As the limb of 2 - $R_2R_2R_2$, 4 - R_2R_2S , and 3 - R_2R_2S mechanisms consists of only two linkages, we select the three mechanisms as the alternative unit. The aerospace mechanism requires high reliability and robustness. The overconstraint mechanism would get stuck because of the interference between the limbs, and the light weight drive cannot provide enough power to overcome the deformation in the mechanism, so it is not the good candidate. Denote M as the number of DOF of the mechanism, n as the number of constraints of the limb, F_O as the number of overconstraints of the mechanism, then for the three kinds of mechanisms, the overconstraint is calculated as follows.

For the mechanism with the limb of $R_2R_2R_2$, it should consist of three limbs in order to have identical load capacity in all directions. Then we have:

$$F_O = 3n - (6 - M) = 3 \times 3 - (6 - 1) = 4 \quad (9)$$

For the mechanism with the configuration of 4 - R_2R_2S , we have:

$$F_O = 4n - (6 - M) = 4 \times 1 - (6 - 2) = 0 \quad (10)$$

For the mechanism with the configuration of 3 - R_2R_2S , we have:

$$F_O = 3n - (6 - M) = 3 \times 1 - (6 - 3) = 0 \quad (11)$$

From the result, we conclude that the 3 - $R_2R_2R_2$ mechanism has four overconstraints, and the other two mechanisms are not overconstrainable. Then we select the mechanisms 3 - R_2R_2S and 4 - R_2R_2S as the unit.

THE OPTIMIZATION OF DEPLOYMENT RATIO

The deployment ratio is the ratio between the length in deployed form and the length in folded form of the feed support mechanism. As the feed support mechanism is composed of the serially connected units, the deployment ratio of the feed support mechanism equals to the ratio between the length in the deployed form and the length in the folded form of the unit, as shown in Fig. 7.

$$\lambda = \frac{l_d}{l_f} \quad (10)$$

where: λ defines the deployment ratio; l_d defines the length in deployed form; l_f defines the length in folded form.

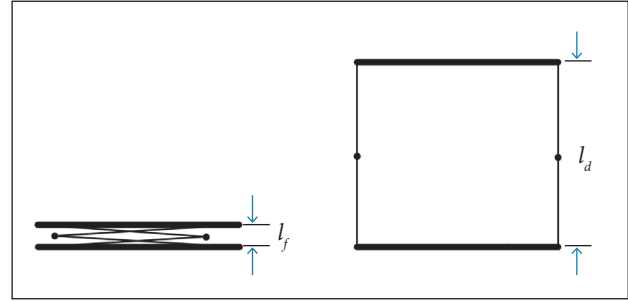


Figure 7. A unit in folded and deployed forms.

The feed support mechanism studied in this paper is limited to the movement in a predetermined cylinder A with radius r . The optimization objective is to find the structure parameters of the unit when it achieves the largest deployment ratio. The schematic diagrams of the two types of parallel mechanisms obtained in the modification and selection of parallel mechanisms are shown in Fig. 8, where θ is the angle between the limb projection and the edge, A is the predetermined cylinder, and α is the angle between the link and the base. When the angle θ changes, the two mechanisms still satisfy their geometric conditions presented in the section about structure synthesis of parallel mechanisms. For the mechanism 3 - R_2R_2S , $0 \leq \theta \leq \pi/6$; for the mechanism 4 - R_2R_2S , $0 \leq \theta \leq \pi/4$.

For the mechanism 3 - R_2R_2S , set $r = 300$ mm. When $\alpha = 0$, the mechanism folds. Set $l_f = 30$ mm. When $\alpha = \pi/2$, the mechanism deploys, and the limb turns into a vertical line. Then $l_d = 2l$, where l defines the link length. The links in the limb should not interfere to each other, as shown in Fig. 9.

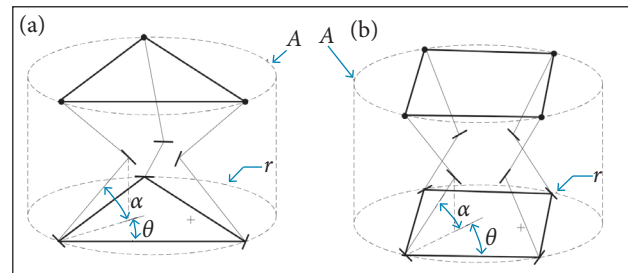


Figure 8. The schematic diagrams of the parallel mechanisms (a) 3 - R_2R_2S and (b) 4 - R_2R_2S .

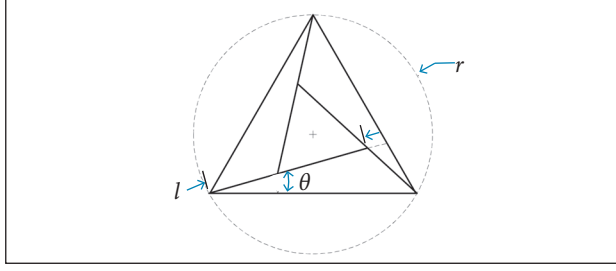


Figure 9. The top view of the mechanism 3 - R_2R_2S .

Then the link length l should follow Eq. 12:

$$l = \frac{\frac{3}{2}(1 - \frac{4}{3}\sin^2 \theta)}{\sin(\frac{\pi}{3} + \theta)} r \quad (12)$$

The deployment ratio $\lambda_{3-R_2R_2S}$ is calculated as:

$$\lambda_{3-R_2R_2S} = \frac{2l}{l_f} = \frac{3(1 - \frac{4}{3}\sin^2 \theta)}{\sin(\frac{\pi}{3} + \theta)l_f} r \quad (13)$$

For the mechanism 4 - R_2R_2S , we set $r = 300$. As in the limbs the two mechanisms are the same, we set $l_f = 30$ mm. Then we take the same process to calculate the deployment ratio as the mechanism 3 - R_2R_2S . The deployment ratio $\lambda_{4-R_2R_2S}$ is shown in Eq. 14:

$$\lambda_{4-R_2R_2S} = 2\sqrt{2} \cdot \frac{1 - \sin^2 \theta}{\cos \theta} \frac{r}{l_f} \quad (14)$$

Calculating λ on the value range of θ , we obtain the relation presented in Fig. 10.

According to Fig. 10, we conclude that, if we choose 3 - R_2R_2S as the unit, when $\theta = 0$, the deployment ratio achieves its largest value; if we choose 4 - R_2R_2S as the unit, when $\theta = 0$, the deployment ratio achieves its largest value. If the cylinder A is predetermined, the mechanism 3 - R_2R_2S has the largest deployment ratio.

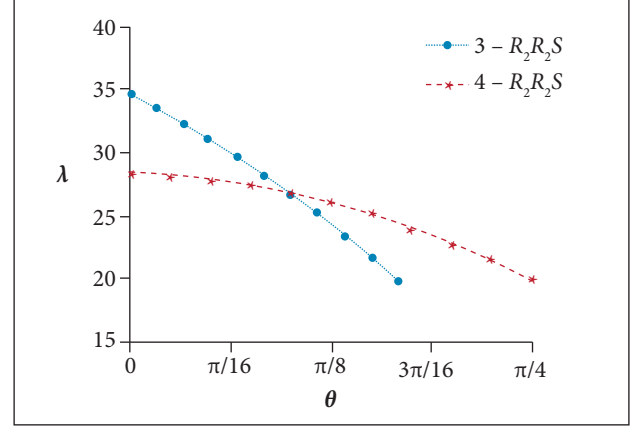


Figure 10. The relation between the deployment ratio λ and θ for mechanisms 3- R_2R_2S and 4 - R_2R_2S .

CONCLUSION

This paper proposes a systematic method to synthesize parallel mechanisms that can be used as feed support mechanisms based on screw theory. To initiate the synthesis, we first study the motion requirement of the feed support mechanisms. Then, three groups of parallel mechanisms are synthesized using the constraint-synthesis method. These mechanisms are then modified according to the practical engineering. Two kinds of parallel mechanisms are selected as the unit for the feed support mechanism. Then the structure parameters of the two kinds of units are optimized, and the mechanism with the largest deployment ratio is obtained. The configurations obtained in this paper can enrich the types of one-dimensional deployable mechanisms in engineering.

ACKNOWLEDGEMENTS

This paper is financially supported by the Natural Science Foundation of China (grant number 51275107) and the “111 Project” (grant number B07018).

REFERENCES

Cherniavsky AG, Gulyayev VI, Gaidaichuk VV, Fedoseev AI (2004). New developments in large deployable space antennae at S.P.A. EGS. Proceedings of the Engineering, Construction, and Operations in Challenging Environments, Earth and Space 2004; Houston, USA.

Fang Y, Tsai L (2002) Structure synthesis of a class of 4-DoF and 5-DoF parallel manipulators with identical limb structures. Int J Robot Res 21(9):799-810. doi: 10.1177/0278364902021009314

Gao F, Yang J, Ge Q (2011) Type synthesis of parallel mechanisms having the second class GF sets and two dimensional rotations. *J Mech Robot* 3(1):011003. doi: 10.1115/1.4002697

Huang Z, Li Q (2002) General methodology for type synthesis of symmetrical lower-mobility parallel manipulators and several novel manipulators. *Int J Robot Res* 21(2):131-145. doi: 10.1177/027836402760475342

Li Q, Huang Z, Hervé M (2004) Type synthesis of 3R2T 5-DOF parallel mechanisms using the Lie group of displacements. *IEEE T Robot Automat* 20(2):173-180. doi: 10.1109/TRA.2004.824650

Merlet JP (2006) *Parallel robots*. 2nd ed. Dordrecht: Springer.

Pour ZA, Shafai L, Tabachnick B (2014) A practical approach to locate offset reflector focal point and antenna misalignment using vectorial representation of far-field radiation patterns. *IEEE T Antenn Propag* 62(2):991-996. doi: 10.1109/TAP.2013.2292503

Sauder JF, Thomson MW (2014). The mechanical design of a mesh Ka-band parabolic deployable antenna (KaPDA) for CubeSats. *AIAA*

2015-1402. *Proceedings of the 2nd AIAA Spacecraft Structures Conference*; Florida, USA.

Silver S (1949) *Microwave antenna theory and design*. New York: McGraw-Hill.

Tayebi A, Gomez J, Gonzalez I, Catedra F (2013) Influence of the feed location on the performance of a conformed Fresnel zone reflector. *IEEE Antenn Wireless Propag Lett* 12:547-550. doi: 10.1109/LAWP.2013.2259460

Tsai LW (1999) *Robot analysis: the mechanics of serial and parallel manipulator*. New York: John Wiley & Sons.

Xu Y, Yao J, Zhao Y (2012) Type synthesis of spatial mechanisms for forging manipulators. *Proc IME C J Mech Eng Sci* 226(9):2320-2330. doi: 10.1177/0954406211433246

Yurduseven, O, Smith D, Pearsall N, Forbes I, Bobor-Oyibo F (2012). A solar parabolic reflector antenna design for digital satellite communication systems. *Proceedings of the 8th IEEE, IET International Symposium on Communication Systems, Networks and Digital Signal Processing*; Poznan, Poland.